Colloids and Surfaces B: Biointerfaces 122 (2014) 662–668

Contents lists available at ScienceDirect

Colloids and Surfaces B: Biointerfaces

journal homepage: www.elsevier.com/locate/colsurfb

Effects of surface wettability on gecko adhesion underwater

Z.L. Peng, C. Wang, S.H. Chen*

LNM, Institute of Mechanics, Chinese Academy of Sciences, Beijing 100190, China

ARTICLE INFO

Article history:
Received 28 April 2014
Received in revised form 20 July 2014
Accepted 27 July 2014
Available online 12 August 2014

Keywords:
Gecko
Adhesion
Surface wettability
Nano-bubble
Capillary force

ABSTRACT

Recent experiments have shown that gecko adhesion underwater depends significantly on surface wettability. Theoretical models of a gecko seta adhering on different substrates are firstly established in order to disclose such an adhesion mechanism. The results show that the capillary force induced by nano-bubbles between gecko seta and the substrate is the mainly influencing factor. The capillary force exhibits an attractive feature between gecko setae and hydrophobic surfaces underwater. However, it is extremely weak or even repulsive on hydrophilic surfaces underwater. A self-similarly splitting model is further considered to simulate multiple gecko setae on substrates underwater. It is interesting to find that the total capillary force depends significantly on the number of nano-bubble bridges and wettability of substrates. The total force is attractive and increases monotonically with the increase of the splitting number on hydrophobic substrates underwater. However, it decreases drastically or even becomes repulsive on hydrophilic substrates underwater. The present result can not only give a reasonable explanation on the existing experimental observations but also be helpful for the design of novel biomimetic adhesives.

1. Introduction

Geckos' amazing adhesion ability had stirred significantly scientific research interests, which could be traced back to the 4th century B.C. [1]. However, until recent decades, extraordinary progresses have been made in understanding how geckos could climb on and detach from almost any surface at will [2–8]. Micro-structures of gecko adhesion system were observed and the fundamental adhesion principle was disclosed experimentally [2,8]. It has been well known that one gecko toe has a lot of lamella structures consisting of thousands of setae and each seta further branches into hundreds of spatulae with nano-scales (5–10 nm in thickness, 200 nm in length and width), typically belonging to a hierarchical structure. Such an adhesion system ensures gecko to obtain strong adhesive force on almost any surface, whether hydrophilic or hydrophobic, rough or smooth [1,2,8].

Experimental and theoretical studies on gecko adhesion mechanisms have been carried out extensively during the past decades, most of which mainly focus on the van der Waals adhesion mechanism on dry solid surfaces [5,8–11]. However, there are more than 1400 species of geckos in the world and different species possess different natural habitats and living conditions [12]. Geckos in tropical rainforests may usually encounter or live on wet surfaces. For example, arboreal geckos like to inhabit on hydrophobic plant surfaces more than other substrates in wet environments [13]. But the van der Waals force is known to decrease drastically in water due to the small Hamaker constant. How do such geckos achieve strong adhesion in wet environments?

Only few literatures have studied the wet adhesion mechanism of geckos so far [14–20]. Huber et al. [14], Sun et al. [16] and Pesika et al. [19] have experimentally proved that capillary force also plays a significant role in gecko adhesion besides the van der Waals force and the adhesive force increases with the increase of relative humidity. However, geckos cannot adhere on hydrophilic glass surfaces once sprayed with water [16,17]. Theoretical analysis of why the relative humidity and sprayed water yield two different effects on gecko adhesion has been investigated in one of our previous works [15]. The disjoining pressure induced by the interlayer water film was found to enhance gecko adhesion. With the increase of relative humidity, water droplets will form and be wrapped by the thin-film-like spatula [21], leading to a drastic decrease of the adhesive force [15].

Recently, systematic experiments of gecko adhesion on different substrates under different conditions have been carried out by Stark et al. [17,18]. It is found that the dry adhesion strength of geckos is extremely strong on both hydrophilic and hydrophobic substrates. When the substrates are submerged in water, gecko adhesion is hardly affected by the aqueous environment, remaining

* Corresponding author. Tel.: +86 10 82543960; fax: +86 10 82543977.
E-mail address: chenshaohua72@hotmail.com (S.H. Chen).

http://dx.doi.org/10.1016/j.colsurfb.2014.07.047
0927-7765/

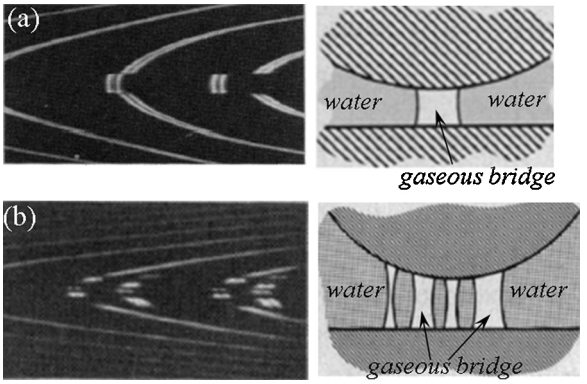

Fig. 1. The interference fringes (left) measured by spectrometer and the deduced interface configuration (right) for two interacting mica surfaces coated with LB (Langmuir–Blodgett) films of hydrocarbon surfactant (a) and fluorocarbon surfactant (b), where the discontinuity in the fringes (left) indicates the vapor-water interface and gaseous meniscus bridging the two contacting surfaces (right).
Source: Taken from H.K. Christenson and P.M. Claesson, Science, 239 (1988), 380–392 [30].

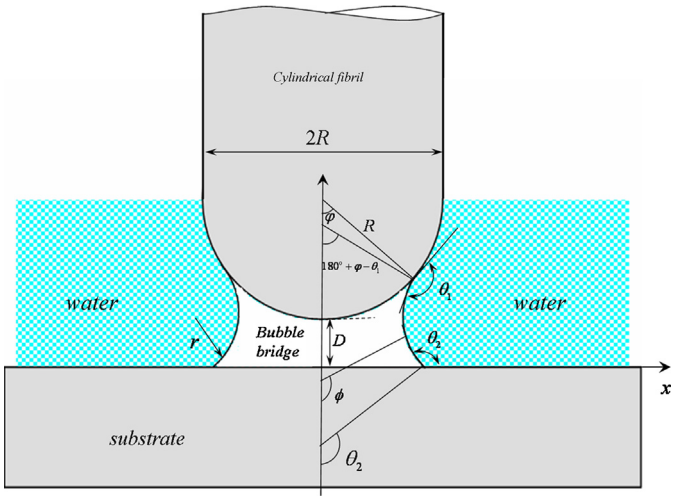

Fig. 2. Schematic of a gecko seta described by a cylindrical fibril with a hemispherical tip in contact with a substrate underwater. A nano-bubble meniscus spontaneously forms at the interface. R is the radius of the fibril and D the separation; φ is the filling angle and ϕ the angle between the normal direction of the meniscus and y axis. θ_1 and θ_2 are contact angles of the fibril and substrate, respectively.

strong adhesion on hydrophobic substrate surfaces, but drastically decreases on hydrophilic ones. Furthermore, it is well known that geckos cannot adhere well on dry polytetrafluoroethylene (PTFE) surfaces due to the extremely small surface energy, which is not true anymore underwater. The adhesive force on a PTFE surface underwater is vastly improved in contrast to the dry case [18,22]. All the phenomena suggest that surface wettability may play a significant role in gecko adhesion underwater.

In fact, the interaction between two hydrophobic surfaces in aqueous environments fascinated many researchers in the last decades due to the strong and inconceivably long-ranged (20–300 nm) attraction [23]. Many possible mechanisms have been proposed, including entropic effects, electrostatic effects, correlated charge fluctuation and nanoscale bubble bridging [24,25]. Most of experiments have shown that cavitations or nano-bubbles can spontaneously form on hydrophobic surfaces as soon as they are brought into water [26–32]. A surprising finding is that nano-bubbles on surfaces are closely packed with a coverage even close to 100%, depending on the chemistry and roughness of surfaces [26,28]. When one hydrophobic surface approaches the other hydrophobic one underwater, they found a strong long-ranged hydrophobic attraction between the two approaching hydrophobic surfaces, which is verified experimentally that the source of the hydrophobic force is due to the coalescence of nano-bubble bridges between them [26–31] as shown in Fig. 1. Due to the superhydrophobicity of gecko's toes [33,34], it is reasonable to infer that nano-bubbles can form on gecko's foot and contribute to gecko adhesion underwater.

Though many experimental investigations have shown the effects of nano-bubble bridges on the long-ranged adhesive force between two hydrophobic surfaces underwater, theoretical studies on such an adhesion mechanism are still lacking [35,36]. Furthermore, what is the possible mechanism of gecko adhesion on substrates underwater? What are the main factors that influence gecko adhesion on wet surfaces? Both questions are unclear and will be answered theoretically in the present paper.

2. A theoretical model of wet adhesion for geckos

2.1. Geometries of gaseous menisci induced by interfacial nano-bubbles

Nano-bubbles can spontaneously form on solid hydrophobic surfaces underwater [26,28–32] and images measured by AFM exhibit that the radius of nano-bubbles usually has an order of magnitude 100 nm, which could coalesce to form a larger gaseous bridge between surfaces [28,30,37]. Fig. 2 shows a gecko seta adhering on a solid surface underwater with a nano-bubble meniscus bridging them. Since the capillary interaction feature between a fiber and a flat substrate does not depend significantly on the fiber's tip shape (flat, cylinder, sphere, etc.) [38–40], gecko seta is modeled as a cylindrical fibril with a hemispherical tip in the present paper for simplicity and without loss of generality [3,4,11,20]. R is the radius of the fibril as well as that of the hemispherical tip. D is the distance between the hemispherical tip and the substrate. φ is the filling angle of the nano-bubble on the hemispherical tip. The contact angle of water on the fibril is θ_1 and that on the substrate surface is θ_2. One should note that the present model with a gaseous meniscus is very similar to the real experimental observations [31,32] and theoretical models with a liquid bridge [20,38,41–44].

The ordinary differential equation describing the profile of the gaseous meniscus can be derived from the Young-Laplace equation as [41–43]

$$\frac{dx}{ds} = \cos\phi, \tag{1a}$$

$$\frac{dy}{ds} = \sin\phi, \tag{1b}$$

$$\kappa = \frac{d\phi}{ds} + \frac{\sin\phi}{x}, \tag{1c}$$

where x and y are coordinates of the axisymmetric meniscus. ϕ is an angle between the normal direction of the meniscus and y axis as shown in Fig. 2. s and κ are the arc length and mean curvature of the nano-bubble profile, respectively.

Boundary conditions of the profile function can be written as

$$\begin{cases} x_1 = R\sin\varphi, \quad y_1 = D + R(1-\cos\varphi), \quad \phi = 180^\circ + \varphi - \theta_1 \\ y_2 = 0, \quad \phi = \theta_2 \end{cases} \tag{2}$$

Eqs. (1) and (2) form a boundary-value problem. It is easy to obtain the profiles of nano-bubble menisci between the fiber and substrates with the help of numerical calculation, which is shown in Fig. 3 for cases of different contact angles and nano-bubble volumes.

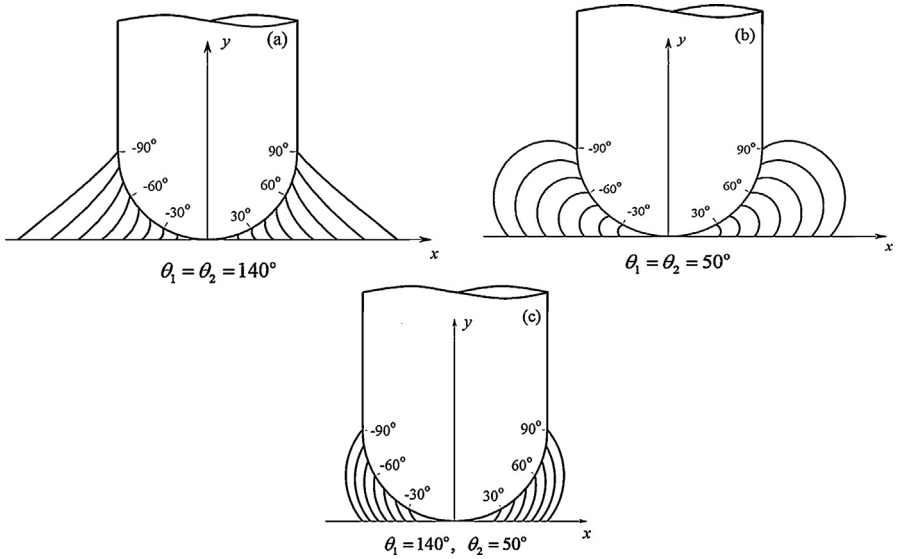

Fig. 3. Geometries of nano-bubble menisci between the fibril and substrate at zero separation with different contact angles and filling angles φ. (a) $\theta_1 = \theta_2 = 140°$; (b) $\theta_1 = \theta_2 = 50°$; (c) $\theta_1 = 140°$, $\theta_2 = 50°$.

2.2. The adhesive force between a gecko seta and a wet substrate

The total adhesive force F between a gecko seta and a wet substrate consists of the nano-bubble capillary force F_c and the van der Waals force F_d,

$$F = F_c + F_d \tag{3}$$

Using the determined geometries of the gaseous menisci (Fig. 3), we can determine the capillary force F_c induced by nano-bubbles. The magnitude of the capillary force depends not only on the surface tension of the gaseous meniscus γ but also on the pressure difference ΔP inside and outside the meniscus. Since the effect of gravity is usually neglected, ΔP is a constant within the meniscus and $\Delta P = \kappa\gamma$ [38]. Then we have

$$F_c = \pi R\gamma \sin\varphi \left[2\sin(\theta_1 - \varphi) - \kappa R \sin\varphi\right] \tag{4}$$

The volume of the nano-bubble bridge can be formulated by the following integral,

$$V = \int_{y_1}^{y_2} \pi x^2\, dx - V_s \tag{5}$$

where V_s is the volume of the hemisphere immersed in the gaseous bubble,

$$\begin{cases} V_s = \dfrac{\pi}{6}(R - R\cos\varphi)\left[3(R\sin\varphi)^2 + R^2(1-\cos\varphi)^2\right], & D \geq 0 \\ V_s = \dfrac{\pi}{6}(R - R\cos\varphi + D)\left\{3R^2\sin^2\varphi + 3\left[R^2 - (R+D)^2\right] + (R - R\cos\varphi + D)^2\right\}, & D < 0 \end{cases} \tag{6}$$

The van der Waals force F_d between a gecko seta and a substrate can be obtained from the classical contact mechanics, which describes essentially the interaction between two solid surfaces. Two alternative contact models are usually adopted, one is the Johnson–Kendall–Roberts (JKR) model for compliant solids with large radii [45] and the other is the Derjaguin–Muller–Toporov (DMT) one for stiff solids with relatively small radii [46]. Since the Young's modulus of gecko setae is relatively high (about 2 GPa) and the scale is relatively small, we adopt the DMT model to describe the dry interaction F_d between the gecko seta and the substrate,

$$F_d = 2\pi R\Delta\gamma \tag{7}$$

where $\Delta\gamma$ is the adhesion energy of the contact interface [20].

3. Results and discussion

3.1. Effect of the contact angle

The wettability of solid surface is usually described by a contact angle. For gecko seta, the contact angle was found to be about $\theta_1 = 128°$ [14], which denotes a hydrophobic characteristic. In fact, the water contact angle on a smooth seta surface (or beta keratin) is about 93°, the "rough" surface of setae (consists of hundreds of spatulae) can greatly increase the apparent contact angle [33]. The effect of the surface wettability on the nano-bubble bridging capillary force between a gecko seta and different substrates is given in Fig. 4, where the distance between the gecko seta and substrates vanishes and different nano-bubble volumes are considered. Contribution of the van der Waals force is also given for comparison with the adhesion energy $\Delta\gamma = 0.01 - 0.05\,\mathrm{J/m^2}$ [11]. Fig. 4 shows that the surface wettability influences the nano-bubble bridging capillary force significantly. In the case of hydrophobic substrates underwater, the gaseous capillary force is strongly attractive and increases with the increase of surface hydrophobicity. Furthermore, the attractive nano-bubble capillary force may be much stronger than the van der Waals force in the case of super-hydrophobic substrates, which shows a dominating gaseous capillary force in gecko adhesion underwater. This finding suggests a possibly strong adhesion for geckos on PTFE surfaces underwater, independent on the weak surface energy of PTFE. Unlike the capillary force of a liquid bridge [20,38], the nano-bubble capillary force decreases with the increase of the surface hydrophilicity under a determined nano-bubble volume, and even becomes repulsive in the case of a seriously hydrophilic substrate. All the results are well consistent with the experimental observations that geckos have strong adhesive force on hydrophobic substrates underwater, but cannot adhere well on hydrophilic ones underwater, for example, glass substrates [17,18]. The findings here also give possible explanations that why arboreal geckos like to inhabit on hydrophobic plant surfaces more than other substrates in wet environments [13].

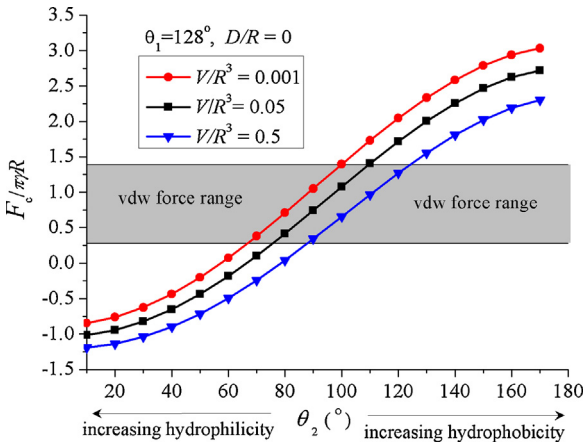

Fig. 4. Effect of the contact angle θ_2 of substrate surface on the nano-bubble capillary force with $\theta_1 = 128^\circ$, $D/R = 0$ and different nano-bubble volumes. The van der Waals interaction is plotted for comparison.

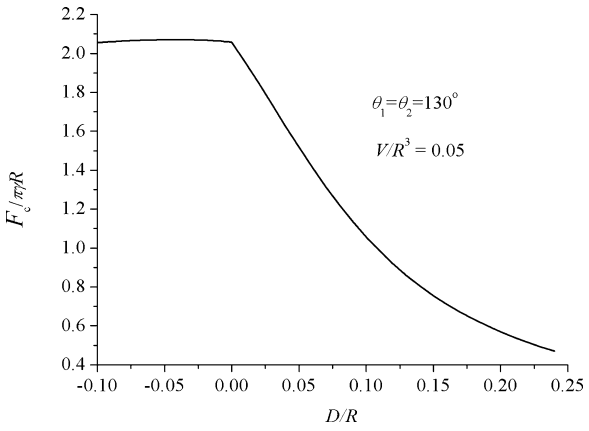

Fig. 5. Variation of the nano-bubble capillary force as a function of the separation with determined contact angles $\theta_1 = \theta_2 = 130^\circ$ and fixed nano-bubble volume $V/R^3 = 0.05$.

3.2. Effect of the separation between a gecko seta and a substrate

In order to further understand some other influence factors of the nano-bubble capillary force, we investigate the effect of the separation between a fibril and a substrate on the gaseous capillary force as shown in Fig. 5, where the contact angles and the non-dimensional nano-bubble volume are taken as $\theta_1 = \theta_2 = 130^\circ$ and $V/R^3 = 0.05$, respectively. It is found that when the separation $D \leq 0$, which denotes a deformed spherical tip completely contacting with a substrate under an external load, the gaseous capillary force almost keeps a constant. While in the case of $D > 0$, the nano-bubble capillary force decreases very quickly with the increase of separation until the nano-bubble meniscus is broken. All the results suggest a robust adhesion mechanism ($D \leq 0$) and easy detachment ($D > 0$) for geckos on a hydrophobic substrates underwater. Therefore, geckos can move freely on a hydrophobic surface without any danger of falling, which is consistent with the natural phenomenon.

3.3. Effect of the nano-bubble volume

Although nano-bubbles can spontaneously form on hydrophobic surface as soon as a substrate is submerged in water, the coverage and volume of nano-bubbles on solid surfaces significantly depend on the physical and chemical properties of the surface, such as wettability, roughness and so on [26,28]. With the help of Eqs. (4) and (5), the dependence of the gaseous capillary force on the volume of nano-bubbles is shown in Fig. 6(a)–(c) for different separations and contact angles.

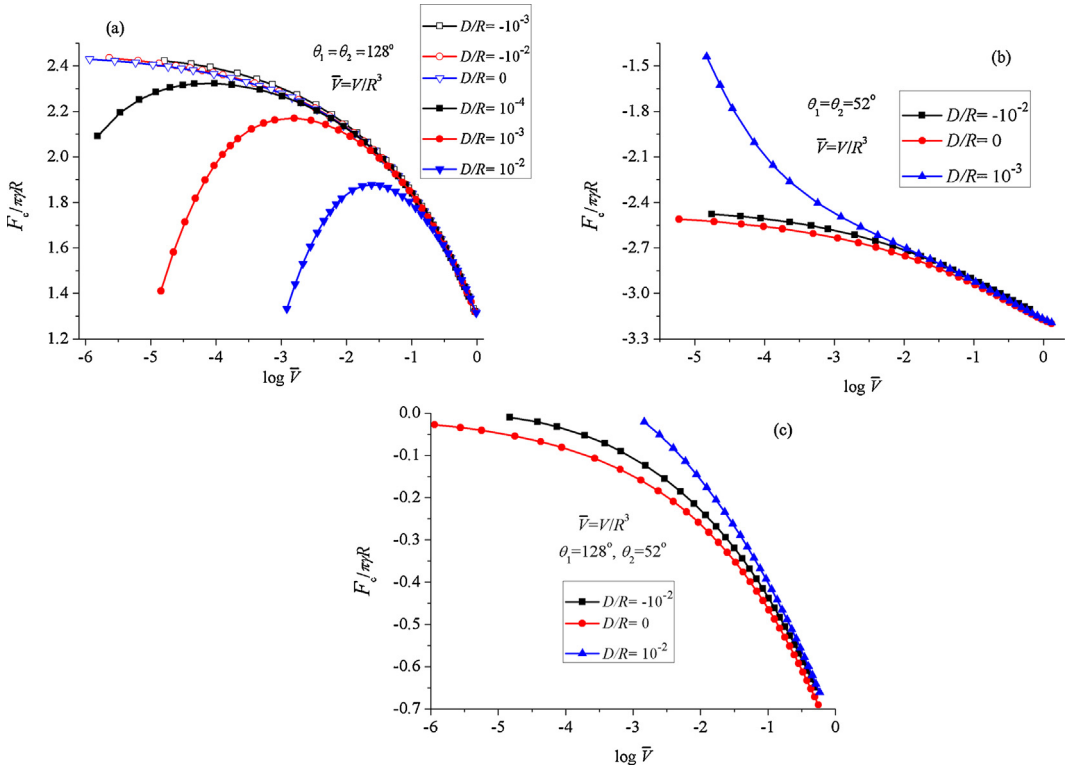

Fig. 6. Nano-bubble capillary force as a function of the nano-bubble volume for different contact angles and separations. (a) for two hydrophobic surfaces $\theta_1 = \theta_2 = 128^\circ$; (b) for two hydrophilic surfaces $\theta_1 = \theta_2 = 50^\circ$; (c) for a hydrophobic surface in contact with a hydrophilic one $\theta_1 = 128^\circ$, $\theta_2 = 52^\circ$.

From Fig. 6(a), one can see that for a wet contact between two hydrophobic surfaces, the gaseous capillary force as a function of the nano-bubble volume varies for different contact distances. When the distance is not larger than zero, i.e., $D \leq 0$, the gaseous capillary force is always decreasing with the increase of nano-bubble volumes. While for the case of $D > 0$, the gaseous capillary force increases first and then decreases after attaining a maximum at a critical nano-bubble volume. With a determined nano-bubble volume, the capillary force is not sensitive to the separation for $D \leq 0$, but decreases seriously with the increase of separation for $D > 0$, which is consistent with the results in Fig. 5. It means a reversible adhesion mechanism could be realized by geckos on a hydrophobic substrate underwater, i.e., strong adhesion ($D \leq 0$) and easy detachment ($D > 0$).

Fig. 6(b) gives the gaseous capillary force as a function of the nano-bubble volume between two hydrophilic surfaces with different separations. It is easy to find that the gaseous capillary force is totally repulsive and the repulsive force increases with the increase of nano-bubble volumes. An interesting phenomenon is that the repulsive capillary force in the case of $D = 0$ is larger than those in the cases of $D > 0$ and $D < 0$. Similar phenomenon can also be found in the model of a hydrophobic surface contacting with a hydrophilic one as shown in Fig. 6(c). In fact, we should note that nano-bubbles can hardly form on a hydrophilic surface spontaneously, especially on a smooth hydrophilic one. Several experiments by AFM have revealed that nano-bubbles on a hydrophilic surface are hardly measured underwater [26,27,47,48]. But if roughness is introduced or solvent-water (i.e. alcohol) exchange method is used in experiments, some nano-bubbles may be formed on a hydrophilic surface [36,49]. Since gecko seta is hydrophobic, nano-bubbles may spontaneously form on it, resulting in gaseous meniscus forming between a gecko seta and hydrophilic substrates underwater. Nevertheless, the repulsive force between a hydrophobic surface and a hydrophilic one underwater suggests the weak adhesion for geckos on a hydrophilic surface, consistent with the experimental observations [17,18]. In addition, it should be noted here, in order to completely understand the mechanical mechanism of capillary force induced by nano-bubbles, we assume artificially nano-bubble bridges also forming between two approaching hydrophilic surfaces in the present paper, which may be not true in reality.

3.4. Effect of multiple nano-bubbles

As we know that gecko adhesion system is a typically multiple fibrillar structure, possessing hundreds of thousands of setae, depending on which geckos realize strong adhesion on substrates. For a dry contact, Artz et al. [5] have successfully studied the effect of multiple fibers on gecko adhesion by splitting one large fibril into many finer fibrils. It was found that the splitting effect could increase significantly the adhesive force in contrast to that of a single large fiber. Chen and Soh [50] studied the adhesion mechanism of a fibrillar structure contacting with an elastic substrate and found that flaw-insensitive adhesion of a fibrillar structure could be achieved by tuning the number and geometrical parameters of fibers. What will be expected for wet adhesion of a multiple fibrillar structure?

Similar to the dry contact model [5], a multiple fibrillar model splitting from a large fiber in contact with a substrate underwater is established with numerous nano-bubble bridges as schematically shown in Fig. 7. The whole volume of gaseous bubbles is V and each small nano-bubble has a volume V/N, where N is the number of splitting finer fibers. Self-similar scaling law results in the radius of each finer hemispherical tip $r = R/\sqrt{N}$ [5]. The total capillary force of the fibrillar adhesion system is the sum of those induced by the N small nano-bubbles.

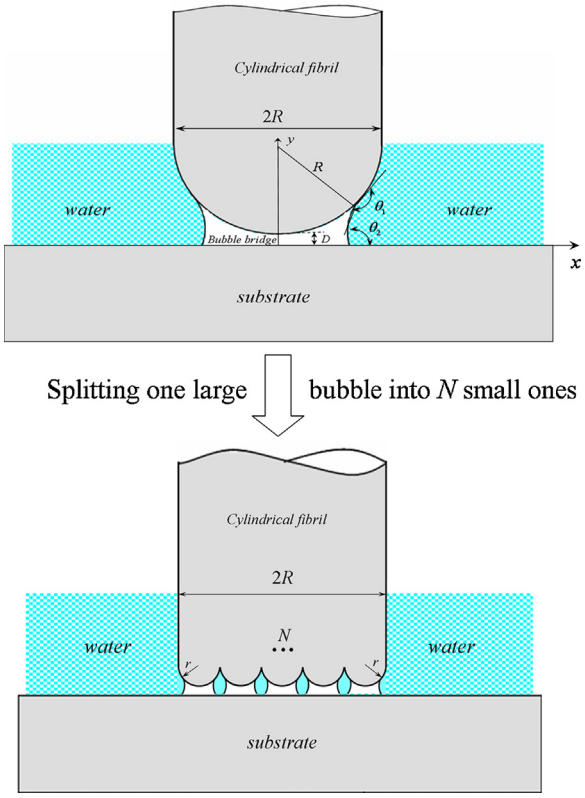

Fig. 7. Schematic of a self-similarly splitting fibrillar structure in contact with a substrate with numerous nano-bubble menisci at interface, in which the total nano-bubble volume and separation between two surfaces keep constants.

Dependence of the total capillary force on the splitting number N is shown in Fig. 8(a)–(c), where the non-dimensionally total nano-bubble volume is fixed to be $V/R^3 = 0.001$ and the separation $D/R = 0$. Fig. 8(a) gives the effect of splitting number on adhesion between two hydrophobic surfaces underwater. From Fig. 8(a), one can see that the total adhesive force increases monotonically with the increase of the splitting number. With a determined number N, the total capillary force decreases with the decrease of contact angles. Results of the case of two hydrophilic surfaces are shown in Fig. 8(b). Obviously, the total adhesive force is repulsive and the splitting number can further improve the repulsive effect. The total adhesive force of a super-hydrophobic surface in contact with different substrates underwater is systematically given in Fig. 8(c), where the contact angle of the super-hydrophobic surface is taken as $\theta_1 = 150^\circ$. It is shown that for a determined splitting number of fibers, the larger the contact angle of the substrate, the larger the adhesive force is. Furthermore, the adhesive force changes from attractive to repulsive when the wettability of substrates varies from hydrophobic to hydrophilic.

Considering the gecko adhesion system, the anti-wetting property of gecko setae as well as the hierarchical structure feature attributes the super-hydrophobic characteristic to gecko foot [33,34]. Thousands of nano-bubbles will spontaneously form on gecko foot underwater. The multiple fibrillar adhesion structure will increase gecko's adhesive force significantly, even on some intermediate hydrophilic substrates as shown in Fig. 8(c). Therefore, the fibrillar structure of geckos can not only enhance the adhesion on dry surfaces [5], but also significantly increase the adhesive force on most of surfaces underwater.

Here, two aspects should be pointed out: (1) All the above analyses of gecko adhesion are conducted with an assumption of

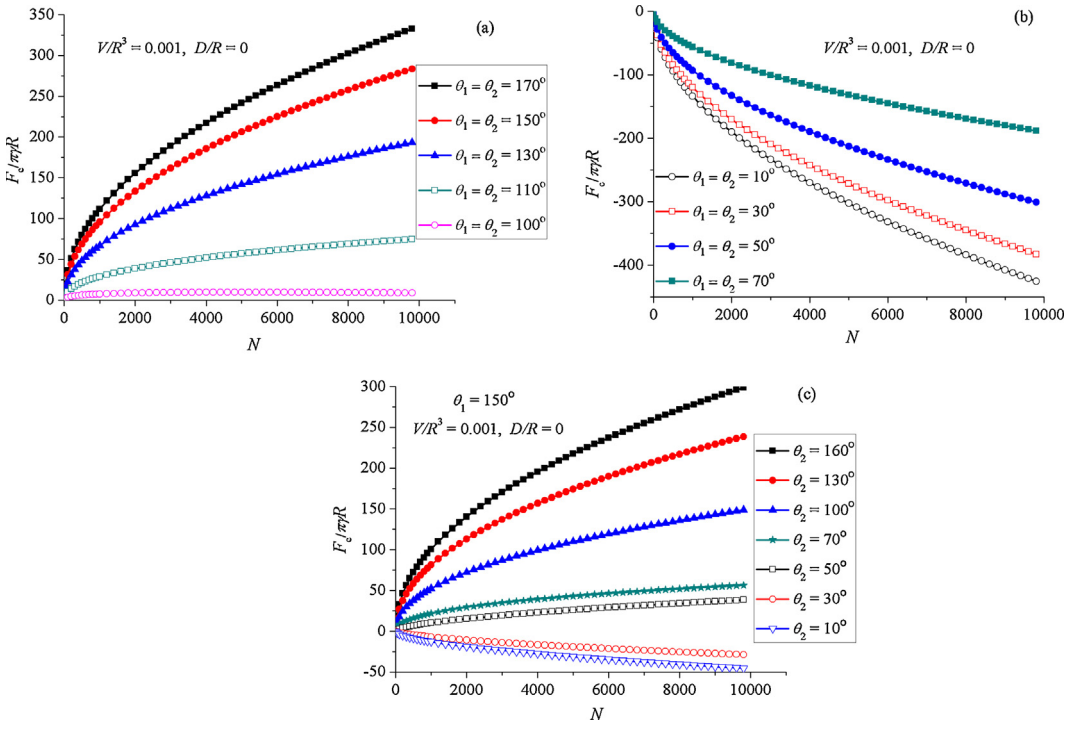

Fig. 8. The total gaseous capillary force of a fibrillar system as a function of the splitting number N with a determined total nano-bubble volume $V/R^3 = 0.001$, separation $D/R = 0$ and different contact angles. (a) for two hydrophobic surfaces; (b) for two hydrophilic surfaces; (c) for a super-hydrophobic surface ($\theta_1 = 150^\circ$) in contact with substrates of different wettability.

initial contact between gecko seta and substrates underwater, and the change of physical properties of gecko seta with the exposure time to water is not considered [17–19]; (2) Only the normal capillary force is considered in the present paper. Whether the interface in the present model could resist shear is not involved. Generally, two contacting surfaces with an interlayer of water cannot resist shear under static loadings except that the thickness of the liquid layer is extremely thin [43]. As for interfaces with liquid or gaseous meniscus bridges, the water coverage is generally smaller than 100%, which ensures some dry contact areas. The ability to withstand shear at the interface depends on the distance between the upper and lower contacting surfaces [3,51,52].

3.5. The stability of nano-bubbles

One of the major issues of the present model is the stability of nano-bubbles underwater. Assuming the diffusion of gas molecules dissolved away from a spherical gas bubble to determine the shrinkage rate, Ljunggren and Eriksson [53] calculated the lifetime of a free gas bubble in water as a function of bubble radius by solving the diffusion equation together with Young-Laplace one. It was found that gas bubbles with radii 10–100 nm had surprisingly short lifetimes about 1–100 μs. It means that a free nano-bubble will instantly dissolve into the surrounding water after formation. However, for a nano-bubble on a solid surface, experimental measurements demonstrated that it could remain for hours or even up to days after its formation [28,54]. Unlike free nano-bubbles underwater, substrate may play a significant role in the lifetime of surface nano-bubbles, which has been further verified theoretically [55]. The pinning of three-phase contact lines on a substrate can significantly slow down the shrinkage of a surface bubble and the inside gas will dissolve with a much longer time than a free spherical bubble underwater [55].

4. Conclusions

Inspired by recent experimental observations, the effect of surface wettability on gecko adhesion underwater is theoretically investigated in the present paper. It is shown that the attractive gaseous capillary force could help geckos to attach strongly on hydrophobic surfaces underwater, while the repulsive capillary force will prevent gecko adhesion on hydrophilic ones underwater. The separation distance between two contacting solids as well as the volume of nano-bubbles also shows significant influence on the interfacial adhesion. Considering the multiple fibrillar feature of gecko adhesion system, a self-similarly splitting model with numerous nano-bubble bridges at interface is further investigated. It is demonstrated that the total capillary force increases monotonically with the increase of the splitting number for cases of hydrophobic surfaces. While it is extremely weak or even repulsive for cases of hydrophilic surfaces and the splitting number in such a case would further improve the repulsive capillary force. The stability of nano-bubbles underwater is also discussed. Unlike the free nano-bubble, the surface nano-bubble is very stable due to the pinning of three-phase contact lines. The present results can not only give a reasonable explanation on the experimental observations, but also be helpful for the design of multi-functional biomimetic devices.

Acknowledgements

The work reported here is supported by NSFC through Grants #11302228, #11125211, #11372317 and the 973 Nano-project (2012CB937500). In addition, the authors give their thanks to the

two anonymous reviewers for their helpful and professional suggestions.

References

[1] K. Autumn, M. Sitti, Y.C.A. Liang, A.M. Peattie, W.R. Hansen, S. Sponberg, T.W. Kenny, R. Fearing, J.N. Israelachvili, R.J. Full, Proc. Natl. Acad. Sci. U.S.A. 99 (2002) 12252–12256.
[2] K. Autumn, Y.A. Liang, S.T. Hsieh, W. Zesch, W.P. Chan, T.W. Kenny, R. Fearing, R.J. Full, Nature 405 (2000) 681–685.
[3] S.H. Chen, H.J. Gao, J. Mech. Phys. Solids 55 (2007) 1001–1015.
[4] S.H. Chen, C. Yan, P. Zhang, H.J. Gao, J. Mech. Phys. Solids 57 (2009) 1437–1448.
[5] E. Arzt, S. Gorb, R. Spolenak, Proc. Natl. Acad. Sci. U.S.A. 100 (2003) 10603–10606.
[6] G. Huber, S.N. Gorb, N. Hosoda, R. Spolenak, E. Arzt, Acta Biomater. 3 (2007) 607–610.
[7] Z.L. Peng, S.H. Chen, Appl. Phys. Lett. 101 (2012) 163702.
[8] Y. Tian, N. Pesika, H.B. Zeng, K. Rosenberg, B.X. Zhao, P. McGuiggan, K. Autumn, J. Israelachvili, Proc. Natl. Acad. Sci. U.S.A. 103 (2006) 19320–19325.
[9] Z.L. Peng, S.H. Chen, Phys. Rev. E 83 (2011) 051915.
[10] Z.L. Peng, S.H. Chen, A.K. Soh, Int. J. Solids Struct. 47 (2010) 1952–1960.
[11] H.J. Gao, X. Wang, H.M. Yao, S. Gorb, E. Arzt, Mech. Mater. 37 (2005) 275–285.
[12] T. Gamble, E. Greenbaum, T.R. Jackman, A.P. Russell, A.M. Bauer, PLoS One 7 (2012) 39429.
[13] K. Koch, B. Bhushan, W. Barthlott, Soft Matter 4 (2008) 1943–1963.
[14] G. Huber, H. Mantz, R. Spolenak, K. Mecke, K. Jacobs, S.N. Gorb, E. Arzt, Proc. Natl. Acad. Sci. U.S.A. 102 (2005) 16293–16296.
[15] Z.L. Peng, S.H. Chen, Colloids Surf. B: Biointerface 88 (2011) 717–721.
[16] W.X. Sun, P. Neuzil, T.S. Kustandi, S. Oh, V.D. Samper, Biophys. J. 89 (2005) L14–L17.
[17] A.Y. Stark, T.W. Sullivan, P.H. Niewiarowski, J. Exp. Biol. 215 (2012) 3080–3086.
[18] A.Y. Stark, I. Badge, N.A. Wucinich, T.W. Sullivan, P.H. Niewiarowski, A. Dhinojwala, Proc. Natl. Acad. Sci. U.S.A. 110 (2013) 6340–6345.
[19] N.S. Pesika, H.B. Zeng, K. Kristiansen, B.X. Zhao, Y. Tian, K. Autumn, J. Israelachvili, J. Phys.-Condens. Matter 21 (2009) 464132.
[20] T.W. Kim, B. Bhushan, J. R. Soc. Interface 5 (2008) 319–327.
[21] C. Py, P. Reverdy, L. Doppler, J. Bico, B. Roman, C.N. Baroud, Phys. Rev. Lett. 98 (2007) 156103.
[22] U. Hiller, J. Bombay, Nat. Hist. Soc. 73 (1976) 278–282.
[23] N. Ishida, M. Sakamoto, M. Miyahara, K. Higashitani, Langmuir 16 (2000) 5681–5687.
[24] E.E. Meyer, K.J. Rosenberg, J. Israelachvili, Proc. Natl. Acad. Sci. U.S.A. 103 (2006) 15739–15746.
[25] P. Attard, Adv. Colloid Interface Sci. 104 (2003) 75–91.
[26] J.W.G. Tyrrell, P. Attard, Langmuir 18 (2002) 160–167.
[27] M.A. Hampton, A.V. Nguyen, Adv. Colloid Interface Sci. 154 (2010) 30–55.
[28] J.W.G. Tyrrell, P. Attard, Phys. Rev. Lett. 87 (2001) 176104.
[29] A. Carambassis, L.C. Jonker, P. Attard, M.W. Rutland, Phys. Rev. Lett. 80 (1998) 5357–5360.
[30] H.K. Christenson, P.M. Claesson, Science 239 (1988) 390–392.
[31] S. Singh, J. Houston, F. van Swol, C.J. Brinker, Nature 442 (2006) 526.
[32] J.L. Parker, P.M. Claesson, P. Attard, J. Phys. Chem. 98 (1994) 8468–8480.
[33] K. Autumn, W. Hansen, J. Comp. Physiol. A. - Neuroethol. Sens. Neural Behav. Physiol. 192 (2006) 1205–1212.
[34] K.S. Liu, J.X. Du, J.T. Wu, L. Jiang, Nanoscale 4 (2012) 768–772.
[35] P. Attard, Langmuir 16 (2000) 4455–4466.
[36] M.A. Hampton, A.V. Nguyen, J. Colloid Interface Sci. 333 (2009) 800–806.
[37] N. Ishida, T. Inoue, M. Miyahara, K. Higashitani, Langmuir 16 (2000) 6377–6380.
[38] S.H. Chen, A.K. Soh, Int. J. Solids Struct. 45 (2008) 3122–3137.
[39] M. Farshchi-Tabrizi, M. Kappl, Y.J. Cheng, J. Gutmann, H.J. Butt, Langmuir 22 (2006) 2171–2184.
[40] H.J. Butt, M. Kappl, Adv Colloid Interface Sci. 146 (2009) 48–60.
[41] F.M. Orr, L.E. Scriven, A.P. Rivas, J. Fluid Mech. 67 (1975) 723–742.
[42] Y.W. Su, B.H. Ji, Y.G. Huang, K.H. Hwang, J. Mater. Sci. 42 (2007) 8885–8893.
[43] J. Qian, H.J. Gao, Acta Biomater. 2 (2006) 51–58.
[44] K.J. Obata, T. Motokado, S. Saito, K. Takahashi, J. Fluid Mech. 498 (2004) 113–121.
[45] K.L. Johnson, K. Kendall, A.D. Roberts, Pro. R. Soc. Lond. A 324 (1971) 301–313.
[46] B.V. Derjaguin, V.M. Muller, Y.P. Toporov, J. Colloid Interface Sci. 53 (1975) 314–326.
[47] A.P. Serro, R. Colaco, B. Saramago, J. Colloid Interface Sci. 325 (2008) 573–579.
[48] R.E. Cavicchi, C.T. Avedisian, Phys. Rev. Lett. 98 (2007) 124501.
[49] M.A. Hampton, B.C. Donose, E. Taran, A.V. Nguyen, J. Colloid Interface Sci. 329 (2009) 202–207.
[50] S.H. Chen, A.K. Soh, J. R. Soc. Interface 5 (2008) 373–382.
[51] K. Autumn, A. Dittmore, D. Santos, M. Spenko, M. Cutkosky, J. Exp. Biol. 209 (2006) 3569–3579.
[52] K. Autumn, N. Gravish, M. Wilkinson, D. Santos, M. Spenko, M. Cutsosky, Integr. Comp. Biol. 46 (2006) E5.
[53] S. Ljunggren, J.C. Eriksson, Colloid Surf. A: Physicochem. Eng. Asp. 130 (1997) 151–155.
[54] X.H. Zhang, A. Quinn, W.A. Ducker, Langmuir 24 (2008) 4756–4764.
[55] X.H. Zhang, D.Y.C. Chan, D.Y. Wang, N. Maeda, Langmuir 29 (2013) 1017–1023.